

## Identifying dependencies among multivariate time series

O. De Feo and C. Carmeli

Laboratory of Nonlinear Systems, School of Computer and Communication Sciences  
Swiss Federal Institute of Technology Lausanne  
CH-1015 Lausanne, Switzerland  
E-mail: oscar.defeo@epfl.ch, cristian.carmeli@epfl.ch

**Abstract** — A new method is proposed to estimate the connectivity among a network of weakly coupled dynamical systems starting from multivariate measures. It resorts to nonlinear modelling of the time series. With simulation examples we demonstrate its adequacy in identifying the direction and the strength of dependencies among observed oscillators.

### 1. Introduction

The problem of inferring the nature of dynamical interactions within a network of dynamical systems is a key topic in several applied sciences. The identification of the direction and the estimation of the strength of such couplings are important toward understanding the mechanisms of interactions and formulation of predictions. Usually, this concerns the estimation of dependencies among multivariate signals (measured time series). Most of the methods assessing directional interdependencies has been proposed for bivariate time series. Typical approaches are measures based on information theory [1], mutual predictability [2], instantaneous phase [3] and time series modelling [4]. The common drawback of measuring the dependence only between two time series is the impossibility of removing the potentially existing effects of a third (or more) series. Recently, two methods, one based on graphical models [5] and one based on mixed state space analysis [6], have overtaken this problem. Whereas the former deals with the stochastic properties of the observed processes, the latter fits into a deterministic framework and, unfortunately, lacks a compact description of the estimated interactions. The method we propose here belongs to the field of multivariate deterministic modelling and does not have this disadvantage. A description of the method will be given in Sec. 2, whilst in Sec. 3 numerical tests will be presented. Conclusions will be given in Sec. 4.

### 2. Method

The method aims at identifying the connectivity matrix of several coupled dynamical systems starting from the measured time series. A reference model of a heterogeneous network of weakly coupled oscillators is assumed. Let denote by  $\Theta$  the state space of the dynamical system

represented by the whole network of oscillators. The reference model (here we assume time to be continuous, but the case of maps is completely analogous) can be written as

$$\dot{\Theta}(t) = \mathcal{H}(\Theta(t)) + \mathcal{G}(\Theta(t)) + \eta, \quad (1)$$

where  $\mathcal{H}(\Theta(t))$  is the dynamics of the oscillators network without the mutual influences, which are in turn modelled by the function  $\mathcal{G}$ , and finally  $\eta$  is the so called “modelling noise”. Under our hypothesis of weak coupling,  $\mathcal{G}$  can be approximated with a linear dependence

$$\mathcal{G}(\Theta(t)) \simeq K\Theta(t), \quad (2)$$

where the matrix  $K$  models the connectivity within the network.

Let us suppose to have a scalar observable from each oscillator, then we can proceed to the estimation of the reference model in three steps.

#### 2.1. First Step — State Space Reconstruction

Let denote by

$$\begin{bmatrix} u_0 \\ \vdots \\ u_t \\ \vdots \\ u_{N-1} \end{bmatrix} \quad u_t \in \mathbb{R}^M \quad (3)$$

the multivariate vector of the measured time series; where  $M$  is the number of observed variables, *i.e.* the number of oscillators, and  $N$  is the number of available samples. By assuming that a local oscillator is behind each scalar variable, at time  $t$  the state space  $x_i(t)$  of the generic oscillator  $i$  can be reconstructed from

$$u_t^i = u(x_i(t)) + v_t, \quad (4)$$

where  $u$  is some measurement function and  $v_t$  the observation noise. The technique we use for this issue is the Principal Component Analysis [7], since it is robust regarding noise. We will denote as  $m_i$  the estimated state space dimension of the generic oscillator  $i$ .

## 2.2. Second Step — Self Modelling

By assuming that the coupling term in Eq. (1), *i.e.*  $\mathcal{G}(\Theta(t))$ , is small with respect to  $\mathcal{H}(\Theta(t))$  such that it can be confused with the modelling noise, *i.e.*  $\eta$ , for every local oscillator  $i$  a model is identified on the base of the solely local measures of the oscillator at issue; we call it “self-model” and we will denote it as  $f_i^s$ . This is done in two sub-steps.

First we obtain the best linear estimation (in a least square sense) of  $f_i^s$ , basically by Moore-Penrose inversion. This corresponds to have

$$f_i^s(x_i(t)) = Ax_i(t) \quad (5)$$

where  $A$  represents the kernel of the image of  $x_i^p(t)$  (the trajectory of the oscillator  $i$  up to time  $t$ ) and the prediction error  $\psi$  given by

$$x_i(t+1) - f_i^s(x_i(t)) = \psi \quad (6)$$

lays in the linear null space of  $x_i^p(t)$  (the prediction error in Fig. 1).

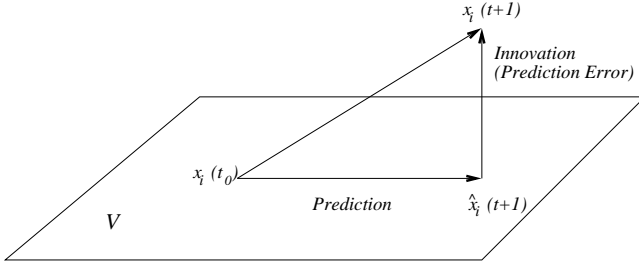


Figure 1: The point  $x_i(t+1)$  of the trajectory at time  $t+1$  (here we assume the prediction step equal to one sample) lays in the state space  $\mathbb{R}^{m_i}$ . Its linear prediction  $\hat{x}_i(t+1)$  given the past trajectory from initial time  $t_0$  to time  $t$  lays on a linear subspace of  $\mathbb{R}^m$ ,  $V = \text{Image}[x_i^p(t)]$ . The difference between  $x_i(t+1)$  and the predicted  $\hat{x}_i(t+1)$  lays in the null space of  $x_i^p(t)$ , which is orthogonal to  $V$  by definition.

If this prediction error does not result to be a stationary gaussian process, we proceed into the second sub-step using Radial Basis function (RBF) for modelling the residual  $\psi$ . RBFs [8] provide the global, empirically based, nonlinear model  $\hat{\psi}$  of the form

$$\hat{\psi}(x_i(t)) = \sum_{n=1}^{j=N_c} w_n \phi(\|x_i(t) - \xi_n\|) \quad (7)$$

where  $\phi(\cdot)$  is the radial basis function,  $\xi_n$  are centres,  $w_n$  the model parameters.

Finally, the identified self-model  $f_i^s$  is given by

$$f_i^s(x_i(t)) = Ax_i(t) + \hat{\psi}(x_i(t)). \quad (8)$$

## 2.3. Third Step — Cross Modelling

The global linear model (connectivity matrix  $K$  in Eq. (2)) of the dynamical interaction among the local oscillators is identified starting from the modelling residual of every  $f_i^s$ , *i.e.* the dynamics unjustified by the local self-models.

Let us denote with  $X_{c,i}$  the reconstructed state space of all the oscillators except the  $i$ -th at issue, *i.e.*

$$X_{c,i}(t) = \begin{bmatrix} x_1(t) \\ \vdots \\ x_{i-1}(t) \\ x_{i+1}(t) \\ \vdots \\ x_M(t) \end{bmatrix} \quad (9)$$

An estimate of  $K_i$ , the linear model justifying the coupling among the oscillator  $i$  and all the others, is computed as the minimum norm pseudo-inverse satisfying

$$x_i(t+1) - f_i^s(x_i(t)) = \hat{K}_i X_{c,i}(t) + \zeta_i, \quad (10)$$

where  $\zeta_i$  lays in the linear null-space of  $X_{c,i}^p(t)$  and represents the total residual modelling noise for the oscillator at issue.

Finally, the estimated global connectivity matrix  $\hat{K}$  is obtained as

$$\hat{K} = \begin{bmatrix} \hat{K}_1 \\ \vdots \\ \hat{K}_i \\ \vdots \\ \hat{K}_M(t) \end{bmatrix} \quad (11)$$

where the  $\hat{K}_i$  have been padded with a matrix of zeros at the suitable position.

The computed matrix  $\hat{K}$  consists of blocks  $C^{i,j}$

$$\hat{K} = \begin{bmatrix} \emptyset & \dots & \dots & C^{1,M} \\ \vdots & \ddots & \ddots & \vdots \\ \vdots & C^{i,j} & \ddots & \vdots \\ C^{M,1} & \dots & \dots & \emptyset \end{bmatrix} \quad (12)$$

of dimension  $m_i \times m_j$ . Every sub-matrix  $C^{i,j}$  represents the strength of the estimated coupling from the state variables of oscillator  $j$  to the ones of oscillator  $i$ . To extract the topology of the influence graph among the oscillators, we coalesce the dependencies between the single state variables by means of the 2-norm estimation of every sub-matrix  $C^{i,j}$ .

### 3. Numerical Examples

The aim of this section is to show two numerical tests. They have been considered for the assessment of the effectiveness of the method previously presented.

As first example, we studied an unidirectionally coupled system composed of two Lorenz oscillators (see Fig. 2). Assuming that oscillator 1 drives oscillator 2, the model for the Lorenz oscillator 2 is described by

$$\begin{cases} \dot{x}_2 = \sigma_2(y_2 - x_2) + \eta_{x_2}, \\ \dot{y}_2 = r_2x_2 - y_2 - x_2z_2 + c^{2,1}(y_1 - y_2) + \eta_{y_2}, \\ \dot{z}_2 = x_2y_2 - b_2z_2 + \eta_{z_2}, \end{cases}$$

where  $\sigma_2$ ,  $r_2$ ,  $b_2$  are parameters,  $\eta_{j_i}$  is modelling random noise (set in the simulations to the reasonable strength of 1% of the energy of the right hand side along the attractor), and the last term in the second equation has been introduced for modelling a (linear) coupling of strength  $c^{2,1}$ . Similarly, the driver's model is described by an autonomous (*i.e.*  $c^{1,2} = 0$ ) system of equations

$$\begin{cases} \dot{x}_1 = \sigma_1(y_1 - x_1) + \eta_{x_1}, \\ \dot{y}_1 = r_1x_1 - y_1 - x_1z_1 + \eta_{y_1}, \\ \dot{z}_1 = x_1y_1 - b_1z_1 + \eta_{z_1}. \end{cases}$$

The differential equations were iterated using the Heun algorithm [9] with  $\Delta t = 0.005$ . This was checked to yield numerically stable results. In order to eliminate transients, the first  $10^4$  iterations were discarded. All time sequences had length  $N = 10^3$ . In order to check for repeatability and stability of results, all computations were repeated several times with different initial conditions. We assumed as measurement the thirds state variables,  $z_1$  and  $z_2$ , with an observational noise of 1% of the signal energy (20 db SNR). The state space of every oscillator was reconstructed using Principal Component Analysis with embedding dimension  $m = 3$ , time delay  $\tau = 0.02$  and window length  $w = 1$ . Within the 2<sup>nd</sup> step of the identification method, the Bera-Jarque parametric hypothesis test for composite normality was used and 800 points were used for the RBF's learning (using a freely available Matlab package [10]). Before the 2-norm estimation, the values of coupling between the

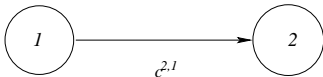


Figure 2: Two Lorenz oscillators (labelled 1 and 2) unidirectionally coupled. The oscillator 1 acts as driver (master) and 2 as response (slave). In the text, we called  $x_i$ ,  $y_i$ ,  $z_i$  ( $i = 1, 2$ ) the state variables of the master and slave system, respectively.

state variables under some suitable relative threshold were set to zero. An estimate of the standard deviation of the obtained coupling values was performed with a generalized cross-validation criterion [11].

For the parameters considered here, the method is able to detect successfully the unidirectional character of the coupling. The result is showed in Fig. 3.

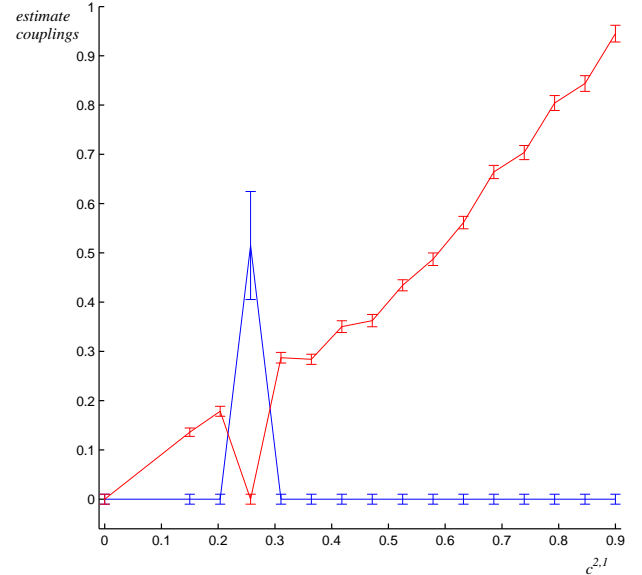


Figure 3: Plot of the estimated mean  $\pm$  standard deviation values of the couplings  $\hat{c}^{2,1}$  (red) and  $\hat{c}^{1,2}$  (blue) as a function of the true unidirectional strength coupling  $c^{2,1}$ . The wrong estimation at  $c^{2,1} \approx 0,21$  is due to a bifurcation occurring in the oscillator 2 when changing the coupling. Furthermore, it should be noted that the variation of this value is bigger than the other ones. This confirms the reliability of the estimated coupling strengths.

In a second example, we have considered a frequently used test: three noisy Lorenz oscillators with unidirectional coupling, arranged in a ring as showed in Fig. 4.

The settings for simulating the temporal behavior of the oscillators and for the identification are the same described in the previous example. We set the coupling strength to the constant values reported in Tab. 1. By taking into account the values reported in Tab. 2, the global-wise estimation of the connectivity correctly reveals the direction and the entity of interaction in the ring structure. On the contrary, using the method for performing a pair-wise analysis as generally done [3], non-existent connections, due to indirect contributions, rise (the elements  $\hat{k}_{3,1}$  and  $\hat{k}_{1,2}$  of the matrix  $\hat{K}$  reported in Tab. 3).

Finally, we can conclude that the two reported examples clearly show that the method is effective in the estimation of both directionality and intensity of the connectivity graph, overcoming the difficulties of a pair-wise analysis.

$$\begin{bmatrix} 0 & 0 & 1.417 \\ 2.075 & 0 & 0 \\ 0 & 2.123 & 0 \end{bmatrix}$$

Table 1: The connectivity matrix  $K$  assigned in the ring structure.

$$\begin{bmatrix} 0.00 & 0.00 & 0.791 \\ 1.719 & 0.00 & 0.00 \\ 0.00 & 1.974 & 0.00 \end{bmatrix} \pm \begin{bmatrix} 0.00 & 0.01 & 0.032 \\ 0.090 & 0.00 & 0.01 \\ 0.01 & 0.032 & 0.00 \end{bmatrix}$$

Table 2: The estimated connectivity matrix  $\hat{K}$  in the ring structure obtained with the global-wise estimation. Mean  $\pm$  standard deviation are reported.

$$\begin{bmatrix} 0.00 & 0.516 & 0.912 \\ 1.623 & 0.00 & 0.00 \\ 0.184 & 1.683 & 0.00 \end{bmatrix} \pm \begin{bmatrix} 0.00 & 0.037 & 0.046 \\ 0.092 & 0.00 & 0.01 \\ 0.008 & 0.096 & 0.00 \end{bmatrix}$$

Table 3: The estimated connectivity matrix  $\hat{K}$  in the ring structure obtained with the pair-wise estimation. Mean  $\pm$  standard deviation are reported.

#### 4. Conclusions

A new method has been proposed for inferring the connectivity matrix of several coupled dynamical systems solely from measured time series. Its capability to discriminate between direct and indirect coupling among the observed dynamical systems has been demonstrated. Therefore, this method has potential applications in several applied science fields where inferring the nature of dynamical interactions is a key problem. For instance, as in population biology is important to know how different populations interact over a given territory, at the same time in neuroscience a key question is how all the single neurons

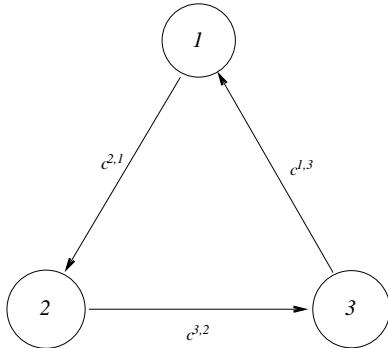


Figure 4: Three oscillators arranged in a ring. The unidirectional (clockwise) coupling is successfully revealed by a multivariate estimation, while a pairwise estimation gives rise to fake connections. See text for details.

treating a certain stimulus make a sense in a whole. Investigations in visual stimuli induced electroencephalographic signals are underway.

#### Acknowledgments

This work was supported by the European Project APEREST: IST-2001-34893 and OFES-01.0456.

#### References

- [1] T. Schreiber, “Measuring information transfer,” *Physical Review Letters*, vol. 85, pp. 461–464, 2000.
- [2] R. Q. Quiroga, J. Arnhold, and P. Grassberger, “Learning driver-response relationships from synchronization patterns,” *Physical Review E*, vol. 61, pp. 5142–5148, 2000.
- [3] M. Roseblum and A. Pikovsky, “Detecting direction of coupling in interacting oscillators,” *Physical Review E*, vol. 64, p. 045202, 2001.
- [4] I. Tokuda, J. Kurths, and E. J. Rosa, “Learning phase synchronization from nonsynchronized chaotic regimes,” *Physical Review Letters*, vol. 88, p. 014101, 2002.
- [5] R. Dahlhaus, “Graphical interactions models for multivariate time series,” *Metrika*, vol. 51, pp. 157–172, 2000.
- [6] M. Wiesenfeldt, U. Parlitz, and W. Lauterborn, “Mixed state space analysis of multivariate time series,” *International Journal of Bifurcation and Chaos*, vol. 11, pp. 2217–2226, 2001.
- [7] D. Broomhead and G. King, “Extracting qualitative dynamics from experimental data,” *Physica D*, vol. 20, pp. 217–236, 1986.
- [8] M. Orr, “Introduction to radial basis function networks,” tech. rep., Centre for Cognitive Science, University of Edinburgh, Edinburgh, Scotland, UK, 1996.
- [9] A. Quarteroni, R. Sacco, and F. Saleri, *Numerical Mathematics*. Springer-Verlag, 2004.
- [10] M. Orr, “Matlab functions for radial basis function networks.” <http://www.anc.ed.ac.uk/~mjo/software/rbf2.zip>, 2001.
- [11] G. Golub, M. Heath, and G. Wahba, “Generalized cross-validation as a method for choosing good ridge parameter,” *Technometrics*, vol. 21, pp. 215–223, 1979.